Robust retrofitting design for rehabilitation of segmental tunnel linings

Zhang, Dong-ming; Zhai, Wu-zhou; Huang, Hong-wei; Chapman, David

DOI:
10.1016/j.tust.2018.09.016

Document Version
Peer reviewed version

Citation for published version (Harvard):
Zhang, D, Zhai, W, Huang, H & Chapman, D 2019, 'Robust retrofitting design for rehabilitation of segmental tunnel linings: using the example of steel plates', *Tunnelling and Underground Space Technology*, vol. 83, pp. 231-242. https://doi.org/10.1016/j.tust.2018.09.016

Robust Retrofitting Design for Rehabilitation of Segmental Tunnel Linings: Using the Example of Steel Plates

Dong-ming Zhang[a], Wu-zhou Zhai[b], Hong-wei Huang[c,*], David Chapman[d]

[a] Assistant Professor, Key Laboratory of Geotechnical and Underground Engineering of Minister of Education and Department of Geotechnical Engineering, Tongji University, Shanghai, China. 09zhang@tongji.edu.cn

[b] Ph.D candidate, Key Laboratory of Geotechnical and Underground Engineering of Minister of Education and Department of Geotechnical Engineering, Tongji University, Shanghai, China. zhaiwuzhou@tongji.edu.cn

[c] Professor, Key Laboratory of Geotechnical and Underground Engineering of Minister of Education and Department of Geotechnical Engineering, Tongji University, Shanghai, China. huanghw@tongji.edu.cn

[b] Professor, School of Civil Engineering, College of Engineering and Physical Sciences, University of Birmingham, Edgbaston, Birmingham, UK. d.n.chapman@bham.ac.uk

Robust Retrofitting Design for Rehabilitation of Segmental Tunnel Linings: Using the Example of Steel Plates

Abstract: This paper presents a general framework for the robust retrofitting design for rehabilitation of segmental tunnel linings installed using shield tunnelling, and specifically using steel plates bonded to the lining as a typical example of such a rehabilitation design. A two-dimensional finite element model is established as part of the robust design which can simulate the deformational response of the steel plates reinforced segmental tunnel lining. The surrounding soil, the tunnel lining, the steel plates and the interactions between each of these are all properly simulated in this model and verified by full-scale test results. The change in horizontal convergence (ΔD_{hs}) subjected to environmental impact, such as unexpected placement of ground surface surcharge is measured to reflect the performance of segmental tunnel linings reinforced by steel plates. The standard deviation of the reinforced tunnel performance due to uncertainties in the soil conditions and the ground surface surcharge is derived to measure the design robustness. A robust rehabilitation design is then accomplished by varying the steel plates sizes (i.e. width and thickness) to maximize the design robustness and minimize the cost using a multi-objective algorithm, also considering the safety requirement constraints. The optimal designs are determined as a set of design points, namely a Pareto Front, which presents a trade-off relationship between the design objectives and is demonstrated as being

useful for decision making. Finally, the robust rehabilitation design method is applied to the retrofitting design of tunnel lining using steel plates in a real case study, and a comparison between the actual design and the design derived by the proposed method has been made to show its applicability and potentially significant advantages for designers, as the method allows consideration of both the highest robustness and the lowest cost simultaneously.

Key words: Robust design, segmental tunnel lining, steel plates, uncertainties, decision making

1. Introduction

The worldwide long-term development of urban metro system has driven the wide use of shield tunneling in construction especially in soft ground. Hence, segmentally lined tunnels installed by shield tunnelling have been utilized for decades, for example London, Tokyo and Shanghai. However, as a typically prefabricated assembled concrete structure, a segmental tunnel lining is vulnerable to nearby disturbance especially in soft ground conditions such as those experienced in Shanghai. Large deformation in terms of transverse convergence and longitudinal settlement, and the associated severe structural defects such as leakage, concrete cracking and spalling have been detected in segmentally lined tunnels from on-site inspection and monitoring data (Shi and Li, 2015; Yuan et al., 2013). The structural health of segmental linings are likely to be adversely affected by nearby engineering activities and human-error related hazards. A typical example was reported by Huang et al. (2017) for a field case study involving an extreme surcharge being applied to a

running metro tunnel in Shanghai. Therefore effective rehabilitation treatments for distressed concrete segmental linings are of great importance, especially at this time of rapid development of shield tunnel construction.

There are several methods suitable for repairing and strengthening segmental tunnel linings, for example bonding fiber reinforced polymer (FRP) or steel plates to the inner surface of segmental concrete linings (Liu and Zhang, 2014; Kiriyama et al., 2005), and grouting on either side of the tunnel at its spring line (Zhang et al., 2014). From these repair measures, bonding steel plates to an existing lining is often chosen as a permanent strengthening method. This rehabilitation approach using bonded steel plates can potentially enhance both the structural stiffness and the ultimate capacity (Kiriyama et al., 2005). Furthermore, the construction operations associated with bonding steel plates can rely on standard machinery resulting in a fast and effective repair procedure. Hence, bonding the steel plates has been successfully adopted as a permanent rehabilitation method in many projects involving damaged segmental tunnel linings worldwide (Chang et al., 2001; Huang and Zhang, 2016).

Kiriyama et al. (2005) presented an analytical analysis for the design of steel plate reinforcement for existing deformed tunnels utilizing a beam spring model. In the model, the steel plates are modelled as a circumferential beam, and a series of nonlinear springs with no tensile resistance are applied in the radial direction to simulate the interaction. Based on the practice of steel plate reinforcement frequently used in Shanghai, Zhao et al. (2015) conducted a full scale load test on a steel plate reinforced segmental lining ring. In their study, a simplified numerical model was

established to further investigate the mechanical and deformational behaviour of reinforced tunnel linings. Apart from these researchers providing insight into the structural response of the lining, other research has focused on the bonding behaviour and failure mode of epoxy bonded steel plate reinforcing concrete structures (Ziraba et al., 1995; Adhikary et al., 2002). Previous literature on numerical simulations provide a basic understanding of the effectiveness of bonding steel plates on the disrupted tunnel structures. However, the model used previously simplified the behaviour of the surrounding soils by using soil springs based on Winkler's model (Do, et al., 2015; Zhang et al., 2017). This simplification will further contribute to any discrepancy between the prediction and the field measurements, especially when the ground conditions are very uncertain in the context of soil properties. Furthermore, the design of steel plate rehabilitation mainly depends on the engineering experience. Hence, an appropriate design model for the rehabilitation of segmental tunnel linings that can be robust appropriate for the environmental uncertainty would be extremely welcome.

A robust design methodology was originally developed by Taguchi & Wu (1979) for improving the industrial product quality and manufacturability. Since then a great many studies have been conducted to understand this idea and make it applicable to other areas. The main idea behind a robust design is to make the system response insensitive to (robust against) hard-to-control disturbances (called noise factors) at a low cost (Kwokleung, 2007). Based on this concept, some researchers have put effort into robust designs of various kinds of structural systems under different uncertainties

105 (Doltsinis and Zhan, 2004; Beer and Liebscher, 2008). In contrast to the design of
106 structures, the geotechnical uncertainty may significantly influence the design
107 associated with geotechnical problems (Phoon and Kulhawy, 1999). Recently, Juang
108 and Wang (2013) proposed a robust geotechnical design (RGD) methodology and
109 applied it to different forms of geotechnical problems such as spread foundations,
110 drilled shafts (Juang et al., 2013) and braced excavations (Juang, et al., 2014). Gong et
111 al. (2014) have applied the robustness design concept for the design of segmental
112 tunnel linings, the idea of this robust design model is to reduce the variation of tunnel
113 lining performance under normal conditions caused by the uncertainty of the input
114 design parameters.

115 The aim of this paper is to present a general framework for the rehabilitation design
116 for segmental linings from shield tunnelling under the conceptual umbrella of
117 robustness. The goal of robust retrofitting design is to enhance the robustness of the
118 reinforced segmental linings against the design uncertainties with consideration given
119 to minimizing cost, which can be accomplished by varying the design parameters to
120 minimize the variation of the reinforced segmental tunnel lining performance given
121 some uncertainty level of the surrounding environments. The general framework for a
122 robust design model is presented first. Secondly a two-dimensional finite element
123 model is established to simulate the steel-plate-reinforced segmental tunnel lining for
124 the design. The interactions between the steel plates and the lining and also between
125 the lining and the surrounding ground are carefully modelled and verified by
126 full-scale load test results. Finally, a detailed design example is carried out

127 demonstrating the applicability of proposed robust design methodology for the
128 rehabilitation of segmental tunnel linings using steel plates.

129 **2. Framework of robust retrofitting design for segmental tunnel linings**

130 **2.1 Practical design method of steel plate strengthening**

131 Figure 1 presents a photograph showing segmental tunnel linings strengthened
132 by steel plates in the Shanghai metro. The steel plates were installed separately and
133 welded together to form an integral ring. Epoxy was injected into the gap and to
134 provide a bond between the lining and the steel plates. Due to the complexity and
135 potentially large differences between the damaged tunnel conditions from case to case,
136 there isn't a common design method for the steel plate rehabilitation method. In fact,
137 the steel plates are usually only applied to damaged tunnel linings with a horizontal
138 convergence of over 10cm. The size of the steel plates used is nearly the same in each
139 case based on past engineering experience, having a width of 850mm and a thickness
140 of 20~30mm. Although this may be convenient in practice, there is certainly room for
141 improvement and optimization in the design of steel plate reinforcement for particular
142 cases.

143 **2.2 Robust retrofitting design methodology**

144 In the robust rehabilitation design procedure, it is aimed to find an appropriate
145 set of design parameters, which makes the performance of reinforced tunnel lining
146 robust enough with the lowest possible total cost. The horizontal convergence is
147 widely adopted as an indicator of tunnel lining performance both in the research field
148 and in engineering practice (Huang and Zhang, 2016). In this study, the change in

149 horizontal convergence (ΔD_{hs}) as a result of an environmental impact such as an
150 unexpected ground surface surcharge, compared to the horizontal convergence ΔD_{h0}
151 just after the steel plate installation has finished is measured to reflect the performance
152 of segmental tunnel lining reinforced by steel plates. However, the change in the
153 convergence ΔD_{hs} as a result of a changed environment will be dependent on multiple
154 sources of uncertainties, for examples the ground properties and the surcharge levels,
155 while the degree of variation in ΔD_{hs} can be quantified by its standard deviation to
156 show how sensitive the reinforced segmental tunnel lining is to the noise factors
157 (Juang et al., 2014).

158 Therefore, the goal of proposed robust retrofitting design is to enhance the
159 robustness of the reinforced segmental tunnel lining against the design uncertainties at
160 low cost, which can be accomplished by varying the design parameters to minimize
161 the standard deviation of the reinforced tunnel performance, ΔD_{hs}, given some
162 uncertainty levels of the surrounding environments. As shown in the flowchart in Fig.
163 3, the robust rehabilitation design procedure is summarized as follows:

164 Step 1: The problem should initially be defined, with the input parameters being
165 divided into two categories, namely the design parameters (*easy to control* factors)
166 and the *noise* factors (*hard to control* factors) (Kwokleung, 2007). The sizes of the
167 steel plates, such as width (w_s) and thickness (t_s) are adopted as the design parameters,
168 as these can be specified by the designers. The *noise* factors are the properties of
169 ground such as soil Young's modulus (E) and environmental impacts, such as the
170 ground surface surcharge (P) in relation to the long-term service life after

171 rehabilitation.

172 Step 2: The uncertainty of the *noise* factors is characterized and the domain of
173 the design parameters is defined. In this study, the uncertainty of these noise factors
174 (i.e. E & P) can be characterized using the data from site investigation information
175 and engineering experience. The domain of the design parameters (i.e. w_s & t_s) is
176 specified by the lower and upper bounds of each design parameters, which can be
177 assigned according to the lining segment dimensions, the limitations of tunnel gauge
178 and engineering experience.

179 Step 3: However, calculating the deformation of the steel-plate-reinforced
180 segmental tunnel lining cannot be solved analytically given the complex interaction
181 problems, and requires numerical simulations. A particular numerical model is
182 established which can simulate the accurate structural response of segmental tunnel
183 linings reinforced by steel plates given certain values of input parameters. The
184 proposed numerical model will be introduced in detail later.

185 In reality, the steel plates are often applied to severely over-deformed tunnels.
186 Based on the statistics of accidents that occurred to the Shanghai metro tunnels
187 (Huang and Zhang, 2016), the unexpected extreme surcharge on ground surface is the
188 most serious factor among all the environmental disturbances causing large tunnel
189 deformations. Thus, the surcharge is selected as the external environmental
190 uncertainty. In the robust rehabilitation design, the surcharge is simulated by applying
191 pressure to the ground surface above the tunnel within the numerical model. The
192 whole numerical analysis procedure is as shown in Fig. 4, for simplification purposes,

193 the steps of the initial geostatic stress equilibrium and tunnelling excavation are not
194 described here, as these have been already finished before this procedure starts. The
195 numerical analysis includes following three steps: (1) The surcharge P_0 is applied and
196 the deformation is recorded before the steel plates are added. The horizontal diameter
197 of the tunnel after this step is denoted as D_{h0}. The specific value of P_0 is determined
198 according to the real tunnel conditions. That is to say, the activation trigger of steel
199 plate and bond spring elements are different from case to case; (2) The steel plate
200 elements and the bond spring elements between the lining and the steel plates are
201 activated in this step to simulate the retrofitting of steel plates to deformed segmental
202 tunnel linings; (3) The surcharge P is continuously applied in this step. The horizontal
203 diameter of the tunnel after this step is denoted as D_h. The change in horizontal
204 convergence of the tunnel after applying the steel plates is then calculated e.g.,
205 $\Delta D_{hs}=D_h - D_{h0}$.

206 Step 4: Based on the proposed numerical model, given the characteristics of the
207 noise factors and specific values for the design parameters, the mean value and
208 standard deviation of the reinforced tunnel performance ΔD_{hs} need to be evaluated.
209 Recalling that a smaller variation in performance (i.e. in terms of the standard
210 deviation) indicates a higher robustness. However, deriving the mean and standard
211 deviation of the tunnel performance is quite variable, as the performance function for
212 such a problem is a numerical model without an explicit function. Thus the five-point
213 point estimate method (5-point-PEM) procedure proposed by Zhao and Ono (2000,
214 2001) is adopted here to estimate the mean and standard deviation of ΔD_{hs}.

Within the proposed 5-point-PEM, the estimating points are obtained in the standard normal space. Therefore the random variables (x_i) need to be transformed into standard normal variables (u_i), which can be easily accomplished by the *Rosenblatt* transformation (Hohenbichler and Rackwitz, 1981). As for a single variable function $y=y(x)$ the mean and standard deviation of y can be calculated as follows:

$$\mu_y = \sum_{j=1}^{m} P_j y\left[T^{-1}\left(u_j\right)\right] \tag{1}$$

$$\sigma_y = \sqrt{\sum_{j=1}^{m} P_j \left(y\left[T^{-1}\left(u_j\right)\right] - \mu_y\right)^2} \tag{2}$$

Where $T^{-1}\left(u_j\right)$ is the inverse *Rosenblatt* transformation, μ_y is the mean value of y, σ_y is the standard deviation of y. The five estimating points in the standard normal space and the corresponding weights are:

$$\begin{aligned} &u_1 = 0; P_1 = 8/15 \\ &u_2 = -u_3 = 1.3556262; P_2 = P_3 = 0.2220759 \\ &u_4 = -u_5 = 2.8569700; P_4 = P_5 = 1.12574 \times 10^{-2} \end{aligned} \tag{3}$$

For a function of multi variables $G = G\left(X\right)$, where $X = x_1, x_2, \cdots, x_n$.

$$G_i = G[T^{-1}(U_i)] \tag{4}$$

Here U_i means u_i is the only random variable with other variables equal to the mean values. The mean and standard deviation of G can be obtained using the following equations:

$$\mu_G = \sum_{i=1}^{n}\left(\mu_i - G_\mu\right) + G_\mu \tag{5}$$

$$\sigma_G = \sqrt{\sum_{i=1}^{n} \sigma_i^2} \tag{6}$$

Where G_μ is the function value when all variables equal to their mean values, μ_i and σ_i are the mean and standard deviation of G_i, which can be obtained using Eqns. (1) and (2). In this study, to evaluate the variation of the reinforced tunnel performance caused by multi sources of uncertainties, ΔD_{hs} could be represented by G, and the parameter variable vector X contains the soil Young's modulus (E_s) and the ground surface surcharge (P). The mean and standard deviation of ΔD_{hs} can be easily calculated by Eqns. (3)-(6). More details of the purposed 5-point-PEM can be found in Zhao and Ono (2000).

Let n denote the number of noise factors, therefore $M=4*n+1$ calculations will be required for one set of design parameters using the proposed 5-point-PEM. This repetition can be achieved by running the ABAQUS numerical analysis automatically in the Matlab environment.

Step 5: In this step, the mean value and standard deviations for each of the N designs in the design space are obtained by repeating the analysis in Step 4.

Step 6: For the purposes of getting the most robust design at low cost, the multi-objective optimization algorithm is carried out to yield the Pareto Front in this step. Thus there are two objectives in the robust rehabilitation design strategy, one is to enhance the robustness of segmental tunnel lining strengthened by steel plates, which can be realized by minimizing the standard deviation of ΔD_{hs}, and the other one is to minimize the rehabilitation cost.

2.3 Cost evaluation

In this study, the total cost of the rehabilitation (C) is made up of two main parts, the cost of the material manufacture (C_m) and the cost of the construction and installation (C_c), which are calculated by following equations:

$$C = C_m + C_c \tag{7}$$

Where C_m can be further calculated from:

$$C_m = p_s \times (2\pi R_i \times w_s \times t_s \times \rho_s) \tag{8}$$

Where p_s is the unit price of the steel; R_i is the inner radius of segmental tunnel lining; w_s is the width of the steel plates; t_s is the thickness of the steel plates; ρ_s is the density of the steel. The unit price of the steel and the construction fee for one ring have been adopted as 30,000 RMB per kilogram and 50,000 RMB respectively, which are based on prices in Shanghai.

2.4 Multi-objective optimization

In step 6 of the robust design procedure, a multi-objective optimization problem is established, as shown in Fig. 5. In this case, the constraints contain the lower and upper bounds of each design parameter. In addition, the safety requirement is also implemented as a constraint by insuring the safety factors f_s above a certain level. In this case, the safety factor f_s ensuring the safety of the segmental tunnel lining reinforced by steel plates is calculated deterministically using equation:

$$f_s = \frac{\Delta D_{\max}}{\Delta D_{hs,mean}} \tag{8}$$

Where $\Delta D_{hs,mean}$ is the mean value of the change in horizontal convergence calculated

275 with all the noise factors being adopted as their mean values. ΔD_{max} denotes the
276 maximum transverse convergence deformation of tunnel lining strengthened by steel
277 plates when the bonding failure occurs, i.e. in this case the value is taken as 26mm as
278 observed in the full-scale test carried out by Zhao et al. (2015). Thus a desired safety
279 level could be ensured by giving a specific limit to the safety factors (f_{sl}).

280 With the confirmed design objectives and constraints, the multi-objective
281 optimization algorithm was performed to seek the optimal design solutions. In the
282 general concept of multi-objective optimization, a set of non-dominated solutions, so
283 called the Pareto Front, is obtained rather than a unique solution optimizing all the
284 objectives. Within the set on the Pareto Front, none of them is better than any other
285 with respect to all the objectives, while the designs in this set are superior to all others
286 in the whole design space. That means, each design in the set on the Pareto Front is
287 optimal, as no improvement could be accomplished in one objective without
288 worsening any other objectives (Gong et al., 2014). In this study, the optimal solutions
289 are obtained by using the Non-dominated Sorting Genetic Algorithm version II
290 (NSGA- II) (Deb et al., 2002). The Pareto Front obtained from this process provides a
291 trade-off relationship between the robustness of the reinforced segmental tunnel lining
292 and the rehabilitation cost. The final design depends on the individual situation, for
293 example if a desired robustness is required, the most economical design could be
294 selected from the Pareto Front. Similarly, if the rehabilitation cost needs to be
295 controlled, the design with the highest robustness level at the given cost limit could be
296 obtained. Furthermore, if there is no specific requirement about the robustness and

297 financial cost, the concept of a knee point may provide the preferred or suggested
298 design within the Pareto Front, which will be explicitly illustrated latter.

299 **3. Numerical modeling**

300 A rational robust design for rehabilitation by using bonding steel plates to shield
301 tunnel lining, as introduced previously, requires a well-established numerical model as
302 a key step in the flowchart. To this end, a two-dimensional finite element model is
303 proposed in this paper for its merit of considering the uncertain soil behaviour and the
304 complex interactions between soils and also between lining and steel plates. The
305 surrounding soil, the tunnel lining, the steel plates and the interactions between each
306 of those are all properly simulated in this model and verified by full-scale test results
307 described in the following sections.

308 **3.1 Establishment of model**

309 A typical two-dimensional finite element model is established using the
310 commercial finite element code ABAQUS as shown in Fig.5. In this model, the tunnel
311 has an outer diameter D_{out} of 6.2m. The mesh size of the entire ground model has a
312 width of 100m and a depth of 50m. The selected mesh width is about 16 times the
313 outer diameter which avoids the effect from the boundary on the calculations (Ding et
314 al., 2004), and the mesh utilizes 4710 elements. The soil is simulated using a linear
315 elastic perfectly-plastic model with a Mohr-Coulomb failure criterion. It is noted that
316 there are a number of soil models that more precisely represent the nonlinear
317 behaviour of soils. However, it could be always argued that the elastic
318 perfectly-plastic soil model with a Mohr-Coulomb yield criteria is probably still the

most widely used in numerical simulations, in particular when there are uncertain soil conditions (Mollon et al., 2011; Do et al., 2013). For the Mohr-Coulomb model, the most critical parameters are soil Young's modulus E_s, Poisson ratio v, soil friction angle φ and cohesion c. The evaluation of these soil parameters is based on the site investigation report. Table 1 shows the magnitude of these parameters used in this analysis. The interaction between the tunnel extrados and the surrounding soils is simulated using the surface-to-surface contact module in ABAQUS.

Details of the simulation used for the steel plate strengthened segmental lining is shown in Fig.7. The lining segments and the steel plates are simulated as different parts, and assembled together in the calculation, as shown in Fig.7 (a). The behaviour of the concrete lining and the steel plates are assumed to be linear elastic perfectly plastic. The properties are given in Table 2. The tunnel segments are modeled using 4-node bilinear elements and the steel plates are modeled using linear planar beam elements. It should be noted that the width and thickness of the steel plates, being *easy to control* factors in the robust design procedure, could be modified by changing the cross section geometry as an input for the beam elements.

Fig. 7 (b) shows details of the radial joint in the numerical model. A surface-to-surface contact is assigned to the interface between the segments, with the coefficient of friction ratio taken as 0.5 (Liu et al., 2014) and the normal behaviour is a hard contact allowing separation. The tensile and shear characteristics of the joints are represented by a tangential spring ($\boldsymbol{k_{j\_\theta}}$) and a radial spring ($\boldsymbol{k_{j\_r}}$). The tangential spring ($\boldsymbol{k_{j\_\theta}}$) is assigned force-deformation relationship as shown in Fig.8 to simulate

the nonlinear behaviour of two grade 5.8 straight bolts with diameter of 30mm and length of 400mm at the longitudinal joint. The stiffness of the radial spring (k_{j_r}) is adopted as 5×10^8N/m (Ding et al., 2004). Hence, the mechanical and deformational behaviour of the longitudinal joint in the tangential, radial and rotational directions could be simulated.

Zhao (2015) proposed a numerical model based on the beam-spring model to investigate the nonlinear response of a segmental lining strengthened by epoxy bonded steel plates. Following their suggestion, the model to simulate the bond behaviour between steel plates and lining incorporates the spring element with normal and shear stiffness, as shown in Fig. 7 (c). The springs allow relative displacement between the connecting nodes in the radial and tangential directions. The shear stiffness and normal stiffness are taken as 6.5 MPa/mm and 60 MPa/mm, respectively, according to the research on epoxy bonded interfaces conducted by Adhikary (2002). Thus the specific stiffness values of the spring elements can be determined according to the element numbers of the spring elements between tunnel lining and steel plates. In this study, 360 pairs of spring elements are distributed uniformly between the lining and steel plates. There are two spring elements in each pair, one in the tangential direction (k_{b_θ}) and the other in the radial direction (k_{b_r}). The stiffness values of the three kinds of linear spring elements, k_{j_r}, k_{b_θ} and k_{b_r} respectively, can be found in Table 3.

3.2 Model validation

The proposed numerical model with the simplifications of the radial joints and

363 bond behaviour between the lining and steel plates needed be validated either via field
364 data from real case study or from a controlled load test before it could be incorporated
365 into the robust design procedure. Due to the limited number of well-documented case
366 studies, a full-scale test carried out by Zhao et al. (2015) is used in this paper. The test
367 results in terms of tunnel convergence subjected to specific load levels are extracted
368 for validation.

369 Since the full-scale load test carried out by Zhao et al (2015) is a purely
370 structural test, the soil continuum in the numerical model is not included in this
371 validation. However, the main simplification in the numerical model is the application
372 of the spring element both for the radial joints and the bonding behaviour between the
373 lining and steel plates. Hence, numerically modelling the load structural test was
374 considered sufficient to validate the rationality for the above assumptions.

375 The test was based on a typical Shanghai metro segmental tunnel lining with
376 15m overburden of soil, the dimension of which was same with that shown in Fig.2.
377 As shown in Fig. 9, 24 point loads were applied to the external surface of the tunnel
378 lining, which were divided into three groups with different values, P1 (6 loading
379 points), P2 (10 loading points), and P3 (8 loading points). The relative displacement
380 between the top and bottom of the tunnel lining ($\Delta D_v=D_v-D_v'$), i.e. called the vertical
381 convergence, was adopted herein as the indicator of overall deformational response of
382 segmental tunnel linings. As illustrated in Fig. 10, there are three steps for the whole
383 loading process: (1) P2=P1×0.65, P3=0.5×(P1+P2), loaded until P2 equals to the
384 passive earth pressure 275kN; (2) P2=275kN, P3=0.5×(P1+P2), loading continued

385 until ΔD_v is approximately 120mm, the steel plate beam elements and bond spring
386 elements are active at this point to simulated the application of the steel plates; (3)
387 P2=275kN, P3=0.5 × (P1+P2), loading then continued until P1=600kN. In the
388 numerical simulations, the load steps and the size of the tunnel lining and steel plates
389 are the same as those used in the test. Further details can be found in Zhao et al.
390 (2015).

391 The calculated deformational responses from the numerical model were extracted
392 and compared to the experimental results. Fig.10 illustrates the vertical convergence
393 (ΔD_v) against P1 from both the full-scale test (dotted line) and the numerical analysis
394 (solid line). The deformation of the segmental lining at two stages, i.e. the initial earth
395 pressure loading and the loading after the bonding of the steel plates are both captured
396 by the loading test and numerical analysis. In the first stage, it is observed from the
397 physical and numerical results that the tunnel deformed nonlinearly with an increase
398 in the surrounding load. Obviously, this is due to the nonlinearity of the joints springs
399 and the geometric nonlinearity of the assembled segmental linings. A maximum
400 difference in P1 between the full-scale test and the numerical analysis is
401 approximately 4.8%, which indicates good agreement even for the largest discrepancy.
402 In the next stage, the deformed segmental linings is reinforced by the steel plates. At
403 this stage the load P1 is shared by both the lining and the steel plates together. An
404 immediately inflection appears right after the reinforcement, as shown in Fig.11,
405 which proves a significant improvement in the stiffness of the segmental lining due to
406 steel plate reinforcement. A maximum difference of 2.9% is observed between the two

results when P1 reaches 580kN. However, it should be noted that the failure of segmental lining reinforced by epoxy bonded steel plates cannot be captured by the proposed numerical model since the bonding springs behave linearly. Although, since there is a good agreement between the two results, it was proposed the numerical model could be used for the subsequent deformation analysis of the segmental lining strengthened by bonded steel plates.

4. Application of robust retrofitting design to a case study

4.1 Case study information

To illustrate the proposed robust retrofitting design methodology, a repair project of an operational shield tunnel disrupted by an extreme surcharge on the ground surface is introduced, and the proposed robust design methodology is applied to the design for steel plate rehabilitation in this case. As reported by Huang and Zhang (2016), and as shown in Fig.12, a large amount of soil was found to be deposited on the ground surface without permission along the alignment of tunnel of the east extension line of the Shanghai metro line 2. The tunnel had been driven through layers consisting typical Shanghai soft clays, i.e. muddy and silty clays. The cross section of the tunnel is the same as that shown in Fig.1, and the longitudinal joints of the segmental lining were arranged in straight lines. The cover depth of this tunnel is 15~20m. The deposited soil had a height ranging from 2m to 7m creating a large surcharge on the ground surface. The segmental tunnel lining underneath this load area was badly damaged, with a large number of defects, such as lining deformation, cracks and water leakage being detected and threatening the safety of the metro

429 operation. Details of the geological conditions and the tunnel information can be
430 found in Huang et al. (2017).

431 As for the emergency response to this accident, a series of rehabilitation methods
432 were applied in the repair work of the damaged tunnel. The lining segment rings from
433 No.500 to No.600 were reinforced using epoxy bonded steel plates. The steel plates
434 had a width of 850mm and thickness of 30mm and were chosen in this case based on
435 practical experience.

436 **4.2 Parameters**

437 The robust design methodology has been subsequently applied to the design of
438 the steel plate rehabilitation for the damaged segmental lined tunnel in this case. The
439 parameters to be used within the numerical model for the proposed design
440 methodology needed to be determined. The properties of the segmental tunnel lining
441 are shown in Table 1. The ground was simplified to homogenous and the
442 geotechnical parameters of the soil were adopted based on the site conditions. As
443 introduced previously, an elastic perfectly plastic constitutive model with a
444 Mohr-Coulomb failure criteria were assigned to the ground soil within the proposed
445 numerical model, with the soil stiffness being indicated by Young's modulus (E_s)
446 while the soil strength was given by friction angle (φ) and cohesion (c). Since the
447 variance in the stiffness parameters was more influential than the strength parameters
448 to the tunnel lining deformation, which was of more interest for the robustness
449 analysis, the friction angle (φ) and cohesion (c) were adopted as deterministic values
450 according to the site investigation given by Huang et al. (2017), while the Young's

451 modulus (E_s) was treated as a random variable following lognormal distribution with
452 a mean of 20MPa and a coefficient of variance (*COV*) of 0.3.

453 The height of the deposited soil within the surcharged area was on average 5m,
454 and assuming that the unit weight of the deposited soil was 20kN/m^3, the value of the
455 surcharge before reinforcement (P_0) was taken as 100kPa. In this case, the surcharge
456 after reinforcement (P) was treated as a random variable following a lognormal
457 distribution with a mean of 50kPa and a *COV* of 0.4, although it should be noted that
458 the characteristic value of P will be different from case to case and should be
459 determined according to the design requirements.

460 As introduced previously, the width w_s and thickness t_s of the reinforcing steel
461 plates are design parameters. Considering the manufacturing convenience of steel
462 plates and engineering experience, the range of w_s was taken from 700mm to 1200mm
463 in increments of 50mm and the range of t_s was taken from 5mm to 30mm in
464 increments of 2.5mm. As for the cost evaluation of steel plate rehabilitation, the
465 construction fee of steel plate rehabilitation for one ring C_c was adopted as 50,000
466 RMB, and the unit price of the steel p_s was adopted as 30,000 RMB/t in this case. As
467 for the safety requirement, the ultimate horizontal convergence of the reinforced
468 segmental lining was adopted as ΔD_{max}, the safety factor (f_s) was limited to be higher
469 than 1.5 to ensure the safety of segmental tunnel linings reinforced with bonded steel
470 plates in the future.

471 **4.3 Parametric analysis**

472 Before conducting the robust design for the rehabilitation of segmental tunnel

473 lining using steel plates, a parametric analysis was conducted to investigate the
474 influence of the noise factors (E_s and P) and the design parameters (w_s and t_s) on the
475 design objectives.

476 In order to illustrate the influence of the soil properties and surcharge value on
477 the segmental tunnel lining performance, the curves of horizontal convergence against
478 surcharge value of tunnel under different conditions are presented in Fig. 13.
479 Comparing the curves for the steel plate reinforced segmental tunnel lining and the
480 one without any treatment, the stiffness is significantly improved due to the
481 reinforcement. For the curves where the soil Young's modulus was taken as mean E_μ,
482 the gradient of curve changes from 1.208 to 6.923, which indicates the stiffness of the
483 reinforced tunnel is 5.7 times higher than that of the tunnel without reinforcement.
484 Moreover, by comparing the curves for all the soil Young's modulus values, i.e.
485 $E_{\mu-\sigma}$, E_μ and $E_{\mu+\sigma}$, it is obvious that the variance in this soil property has an impact on
486 the horizontal convergence. Nevertheless the degree of variation is significantly
487 reduced due to the steel plates, which means the robustness of the segmental tunnel
488 lining could be enhanced to a large degree by bonding steel plates to it.

489 For the purposes of showing how the design parameters influence the robustness
490 and cost of segmental tunnel lining reinforced by steel plates, the relationship between
491 sizes of steel plates and design cost and robustness are presented in Fig. 14. It is
492 evident that the standard deviation decreases with increase in the steel plate width (w_s)
493 or thickness (t_s). In addition, comparing the design with w_s=1000mm and t_s=20mm in
494 Fig.14 (a) and the design with w_s=800mm and t_s=25mm in Fig.14 (b), the calculated

costs of the steel plate rehabilitation are both 131,340 RMB, while the standard deviation (std) of ΔD_{hs} are 1.864 and 1.816 respectively. The cost of the two designs are the same, however the latter one shows a higher level of robustness. This means that the increase in investment could bring about a higher level of robustness, however, the robustness may sometimes be different even with for same cost. Therefore, the optimization shows its importance within the robust design procedure.

4.4 Robust retrofitting design

In this example of the robust retrofitting design procedure, the elastic modulus of soil (E_s) and the surcharge after reinforcement (P) are the noise factors, while height (w_s) and thickness (t_s) of reinforcing steel plates are the design parameters. From the parameters introduced previously, the design constraints can be confirmed to include the lower and upper bound of the design parameters and the safety requirement. One of the design objectives is to maximize the design robustness by minimizing the standard deviation of ΔD_{hs}, however, the other one is to minimizing the cost of the steel plate rehabilitation. Thus the process of the robust design for rehabilitation of segmental tunnel linings using steel plates is carried out as a multi-objective optimization problem as illustrated in Fig. 15. The Non-dominated Sorting Genetic Algorithm version II (*NSGA- II*) (Deb et al., 2002) has been employed to obtain the Pareto Front for the established multi-objective model.

As shown in Fig. 16, the Pareto Front obtained using NSGA- II is marked as hollow circles within the two-dimensional coordinates, where two objectives, the standard deviation of ΔD_{hs} and cost, are in x and y axes respectively. Within the

517 obtained Pareto Front, it is obvious that the robustness tends to increase as the total
518 cost increases, which means that increasing the investment can significantly improve
519 the design robustness. Between all these designs on the Pareto Front, none of them is
520 better than any other in all the objectives, which offers a trade-off relationship
521 between to objectives of robustness and cost. It should be noted that, all the designs
522 on the Pareto Front satisfy the safety requirement.

523 The obtained designs in the existing Pareto Front are such that a choice of the
524 most optimal single design is not straightforward. Thus engineers need make decision
525 with the help of the trade-off relationship between design robustness and cost.
526 However, the most preferred or recommended design named the 'knee point' can be
527 obtained in such a bi-objective problem by using a multi-criteria decision making
528 methodology (Kalyanmoy and Shivam, 2011). A knee point is almost the most
529 preferred design, since a small improvement in any one objective requires an
530 unfavorably large sacrifice in another. The normal boundary intersection method has
531 been adopted herein to locate the knee point on the obtained Pareto Front (Das 1999;
532 Juang et al., 2014). In this method, as shown in Fig. 16, two extreme points A and B
533 are obtained to construct the boundary line $L(A,B)$. Subsequently, for each design
534 point on the Pareto Front, the distance from the boundary line $L(A,B)$ can be
535 calculated. Thereafter, the design point with the maximum distance from the boundary
536 line $L(A,B)$ is defined as the knee point. In this example, the knee point has the
537 following parameters: w_s=750mm, t_s=15mm with a cost of 9.575×10^4 RMB. Above
538 this level, a small improvement in robustness may need a large involvement. While

539 below this level, a slight cost decrease will significantly reduce the design robustness.

540 In Fig. 17, design 1 represents the actual design in this case, designs 2 and 3 are
541 the two design point within the obtained Pareto Front, and design 4 is the design
542 yielded by using concept of the knee point. A comparison of these four designs is
543 shown in Table 4. Compared with design 1, the robustness of design 2 is enhanced
544 with little increase in cost, while design 3 yields almost the same robustness with a
545 lower cost. Although the robustness of design 4 is lower than that of design 1, the cost
546 saving is large. Therefore, the significance of the robust retrofitting design proposed
547 in this paper is that the design can be carried out considering both the highest
548 robustness and the lowest cost simultaneously.

549 **5. Conclusion**

550 This paper has presented a general framework for the robust retrofitting design
551 methodology of segmental lined tunnel of shield tunnels using steel plates. The goal
552 of the proposed design methodology is to enhance the robustness of the reinforced
553 segmental tunnel lining against the design uncertainties with respect to achieving low
554 cost, which can be accomplished by varying the design parameters to minimize the
555 variation of the reinforced tunnel performance given some uncertain level in
556 surrounding environments. Specifically, the bonding of steel plates to the lining is
557 selected as a typical example of such a kind of rehabilitation design discussed in this
558 paper. The general framework of the robust design method is initially presented. Then
559 a two-dimensional finite element model is established to simulate the steel plates
560 retrofitting for deformed segmental tunnel linings. The interactions between the steel

561 plates and the lining and also between the lining and the ground soil are carefully
562 modelled and verified by the full-scale load test results. Finally, a detailed design
563 example is carried out for the applicability of the purposed robust design methodology
564 for rehabilitation of segmental tunnel linings by using steel plates. The results
565 presented in this paper demonstrate the significant potential of utilizing the robust
566 retrofitting design methodology combined with the multi-objective optimization
567 technique where decisions involve different design options and cost. The following
568 conclusions can be draw:
569 (1) The proposed numerical model was able to simulate the steel plate reinforcement
570 procedure and the structural response of segmental tunnel linings. The deformation of
571 the segmental linings develops nonlinearly with an increase in surcharge loading on
572 the ground surface. The overall stiffness of the segmental lining can be significantly
573 improved due to the installation of steel plates. The uncertainties existing in the
574 surrounding environment, e.g. the soil conditions and the ground surface surcharge,
575 may cause a variation in the performance of the reinforced segmental tunnel lining.
576 (2) The concept of the robust retrofitting design methodology is introduced in this
577 article, where in this case the design is considered to be robust if the reinforced tunnel
578 performance is insensitive to the variation in the noise factors (in this case, the soil
579 conditions and ground surcharge). The proposed design method is accomplished by
580 varying the design parameters to minimize the standard deviation of reinforced tunnel
581 performance and the cost simultaneously using a multi-objective optimization
582 algorithm.

583 (3) The Pareto Front derived from the multi-objective optimization reveals trade-off
584 relationships between the design robustness and the rehabilitation cost. Comparing all
585 the designs within the obtained Pareto Front, none is better than any other in
586 achieving all the objectives, and the engineer can make decisions with respect to their
587 own financial restraints or robustness goals. Nevertheless, the most preferred or
588 recommended design could be pointed out with the concept of the knee point.
589 It should be noted that the robust retrofitting design methodology presented in this
590 paper is a potentially powerful tool that can be applied not only for tunnel linings, but
591 also for other underground or above ground structures. However, the details may be
592 different from case to case. For example, the standard deviation of the tunnel
593 transverse deformation is adopted to indicate the sensitivity to the noise factors in this
594 paper, while the appropriate sensitivity index needs to be selected for a different
595 problem. In addition, in this paper the retrofitting cost is calculated according to the
596 volume of reinforcing steel plate. However, the evaluation of the retrofitting cost may
597 be more precisely represented in other situations by considering the influence of, for
598 example, time. Therefore, further investigation needs to be conducted when adopting
599 this method for solving other geotechnical or structural problems.

600 **Acknowledgements**

601 This study is substantially supported by the Natural Science Foundation Committee
602 Program (No. 51538009, 51608380), by Shanghai Rising-Star Program
603 (17QC1400300), by International Research Cooperation Project of Shanghai Science
604 and Technology Committee (No. 15220721600), by the Shanghai Science and

605 Technology Committee Program (No. 17DZ1204205) and by Peak Discipline
606 Construction on Civil Engineering of Shanghai Project. Hereby, the authors are
607 grateful to these programs.

608

609 **Reference:**

610 Abaqus. Abaqus User's Manual, Version 6.10. Dassault Systèmes, 2010

611 Adhikary, B. B., & Mutsuyoshi, H., 2002. Numerical simulation of steel-plate strengthened
612 concrete beam by a non-linear finite element method model. Construction & Building
613 Materials, 16(5), 291-301.

614 Beer, M., & Liebscher, M., 2008. Designing robust structures – a nonlinear simulation based
615 approach. Computers & Structures, 86(10), 1102-1122.

616 Chang, C. T., Sun, C. W., Duann, S. W., & Hwang, R. N., 2001. Response of a taipei rapid
617 transit system (trts) tunnel to adjacent excavation. Tunnelling & Underground Space
618 Technology, 16(3), 151-158.

619 Chang, C. T., Wang, M. J., Chang, C. T., & Sun, C. W., 2001. Repair of displaced shield
620 tunnel of the taipei rapid transit system. Tunnelling & Underground Space Technology,
621 16(3), 167-173.

622 Das, I., 1999. On characterizing the "knee" of the pareto curve based on normal-boundary
623 intersection. Structural Optimization, 18(2-3), 107-115.

624 Deb, K., Pratap, A., Agarwal, S., & Meyarivan, T., 2002. A fast and elitist multiobjective
625 genetic algorithm: nsga-ii. IEEE Transactions on Evolutionary Computation, 6(2),
626 182-197.

627 Ding, W. Q., Yue, Z. Q., Tham, L. G., Zhu, H. H., Lee, C. F., & Hashimoto, T., 2004. Analysis
628 of shield tunnel. International Journal for Numerical & Analytical Methods in
629 Geomechanics, 28(1), 57-91.

630 Doltsinis, I., & Zhan, K., 2004. Robust design of structures using optimization methods.
631 Computer Methods in Applied Mechanics & Engineering, 193(23–26), 2221-2237.

632 DGJ08-11, 2010. Shanghai foundation design code (DGJ08-11-2010). Shanghai: Shanghai
633 Construction Committee. (in Chinese).

634 Do, N. A., Dias, D., Oreste, P., & Djeran-Maigre, I., 2013. 2D numerical investigation of
635 segmental tunnel lining behavior. Tunnelling & Underground Space Technology, 37(6),
636 115-127.

637 Do, N. A., Dias, D., Oreste, P., & Djeran‐Maigre, I. 2015. A new numerical approach to the
638 hyperstatic reaction method for segmental tunnel linings. International Journal for
639 Numerical & Analytical Methods in Geomechanics, 38(15), 1617-1632.

640 Gong, W., Wang, L., Juang, C. H., Zhang, J., & Huang, H., 2014. Robust geotechnical design

641 of shield-driven tunnels. Computers & Geotechnics, 56(1), 191-201.
642 Gong, W., Huang, H., Juang, C. H., Atamturktur, S., & Brownlow, A., 2014. Improved shield
643 tunnel design methodology incorporating design robustness. Canadian Geotechnical
644 Journal, 52(10), 150226181849001.
645 Hohenbichler, M., and Rackwitz, R., 1981. ‘‘Non-normal dependent vectors in structural
646 safety.’’ J. Engrg. Mech., ASCE, 107(6), 1227–1238.
647 Huang, H. W., & Zhang, D. M., 2016. Resilience analysis of shield tunnel lining under
648 extreme surcharge: characterization and field application. Tunnelling & Underground
649 Space Technology, 51, 301-312.
650 Shao, H., Huang, H. W., Zhang, D. M., & Wang, R. L., 2016. Case study on repair work for
651 excessively deformed shield tunnel under accidental surface surcharge in soft clay.
652 Chinese Journal of Geotechnical Engineering. (in Chinese)
653 Huang, H.W., Shao, H., Zhang, D., & Wang, F., 2017. Deformational responses of operated
654 shield tunnel to extreme surcharge: a case study. Structure & Infrastructure Engineering,
655 1-16.
656 Juang, C. H., & Wang, L., 2013. Reliability-based robust geotechnical design of spread
657 foundations using multi-objective genetic algorithm. Computers & Geotechnics, 48(4),
658 96–106.
659 Juang, C. H., Wang, L., Liu, Z., Ravichandran, N., Huang, H., & Zhang, J., 2013. Robust
660 geotechnical design of drilled shafts in sand: new design perspective. Journal of
661 Geotechnical & Geoenvironmental Engineering, 139(12), 2007-2019.
662 Juang, C. H., Wang, L., Hsieh, H. S., & Atamturktur, S., 2014. Robust geotechnical design of
663 braced excavations in clays. Structural Safety, 49, 37-44.
664 Phoon, K. K., & Kulhawy, F. H., 1999. Characterization of geotechnical variability.
665 Foundation Engineering in the Face of Uncertainty@sHonoring Fred H. Kulhawy (Vol.36,
666 pp.612-624). ASCE.
667 Kiriyama, K., Kakizaki, M., Takabayashi, T., Hirosawa, N., Takeuchi, T., & Hajohta, H., et al.,
668 2005. Structure and construction examples of tunnel reinforcement method using thin steel
669 panels. Nippon Steel Technical Report (92), 45-50.
670 Kasper, T., & Meschke, G., 2006. A numerical study of the effect of soil and grout material
671 properties and cover depth in shield tunnelling. Computers & Geotechnics, 33(4-5),
672 234-247.
673 Kwokleung Tsui., 2007. An overview of taguchi method and newly developed statistical
674 methods for robust design. Iie Transactions, 24(5), 44-57.

675 Kalyanmoy Deb, & Shivam Gupta., 2011. Understanding knee points in bicriteria problems
676 and their implications as preferred solution principles. Engineering Optimization, 43(11),
677 1175-1204.
678 Liu, Z., & Zhang, D., 2014. The mechanism and effects of afrp reinforcement for a shield
679 tunnel in soft soil. Modern Tunnelling Technology, 51(5), 155-160.
680 Liu, C., Zhang, Z., & Regueiro, R. A., 2014. Pile and pile group response to tunnelling using a
681 large diameter slurry shield – case study in shanghai. Computers & Geotechnics, 59(59),
682 21-43.
683 Mollon, G., Dias, D., Soubra, A. H., & Asce, M. 2011. Probabilistic analysis of pressurized
684 tunnels against face stability using collocation-based stochastic response surface method.
685 Journal of Geotechnical & Geoenvironmental Engineering, 137(4), 385-397.
686 Ministry of Construction of the People's Republic of China (MCPRC). Code for design of
687 strengthening concrete structure (GB50367-2013). China Building Industry Press; 2013 [in
688 Chinese].
689 Shi, P., & Li, P., 2015. Mechanism of soft ground tunnel defect generation and functional
690 degradation. Tunnelling & Underground Space Technology, 50, 334-344.
691 Taguchi, G., & Wu, Y. I. (1979). Introduction to off-line quality control system. Journal of
692 Food Protection, 51(6), 449-451(3).
693 Yuan, Y., Jiang, X., & Liu, X., 2013. Predictive maintenance of shield tunnels. Tunnelling &
694 Underground Space Technology, 38(3), 69–86.
695 Ziraba, Y. N., & Baluch, M. H., 1995. Computational model for reinforced concrete beams
696 strengthened by epoxy bonded steel plates. Finite Elements in Analysis & Design, 20(4),
697 253-271.
698 Zhao, Y. G., & Ono, T., 2000. New point estimates for probability moments. Journal of
699 Engineering Mechanics, 126(4), 433-436.
700 Zhao, Y. G., & Ono, T., 2001. Moment methods for structural reliability. Structural Safety,
701 23(1), 47-75.
702 Zhang, D. M., Zou, W. B., & Yan, J. Y., 2014. Effective control of large transverse
703 deformation of shield tunnels using grouting in soft deposits. Chinese Journal of
704 Geotechnical Engineering, 36(12), 2203-2212.
705 Zhang, D.M, Phoon, K. K., Hu, Q.F., & Huang, H.W., 2017. Nonlinear subgrade reaction
706 solution for circular tunnel lining design. Canadian Geotechnical Journal. DOI:
707 https://doi.org/10.1139/cgj-2017-0006 (online).
708 Zhao, H., Liu, X., Bao, Y., Yuan, Y., & Bai, Y., 2015. Simplified nonlinear simulation of

709 shield tunnel lining reinforced by epoxy bonded steel plates. Tunnelling & Underground
710 Space Technology, 51, 362-371.

711

Table and Figure Captions

Tables:

Table 1 Properties of soil

Table 2 Parameters for the segmental tunnel concrete lining and steel plates

Table 3 The stiffness values of the spring elements simulating the segmental joints and epoxy bonding behaviour

Table 4 Comparison between the actual design and the optimal designs derived by the robust retrofitting design methodology

Figures:

Figure 1 Photograph of a steel plates reinforced segmental tunnel lining

Figure 2 Diagram of showing an example of segmental tunnel linings reinforced by steel plates

Figure 3 Flowchart for developing a robust retrofitting design

Figure 4 Numerical analysis procedure

Figure 5 Multi-objective optimization formulation for robust retrofitting design

Figure 6 Finite element mesh for the ground

Figure 7 Finite element model for steel plates reinforced segmental linings, (a) the 2D model for the full reinforced tunnel lining, (b) the radial lining joint, (c) modelling the bond between the steel plates and the lining segment

Figure 8 Force-deformation relationship assigned to tangential spring in the segment joint

734 Figure 9 Schematic of the applied loading

735 Figure 10 The loading process for P1, P2 and P3

736 Figure 11 Comparison between the full-scale test results and the numerical analysis

737 results

738 Figure 12 Location of the surcharge area

739 Figure 13 Curves showing the horizontal convergence (ΔD_h) against surcharge value

740 Figure 14 Influence of steel plate size on cost and robustness, (a) influence of steel

741 plate width (w_s), (b) influence of steel plate thickness (t_s)

742 Figure 15 Formulation of the robust design for the rehabilitation of segmental tunnel

743 linings using steel plates

744 Figure 16 Pareto front obtained using NSGA-II

745 Figure 17 Comparison between the actual design and the optimal designs on the

746 Pareto Front

747

748

749 Table 1 Properties of soil (Huang et al., 2017)

Parameters	**Symbol**	**Unit**	**Value (or mean value)**	**COV**	**Distribution**
Poisson's ratio	v	-	0.167	-	-
Unit weight	γ	kN/m^3	18	-	-
Cohesion	c	kPa	15	-	-
Friction angle	φ	°	15	-	-
Young's modulus	E_s	MPa	20	0.3	Lognormal

750

751

752 Table 2 Parameters for the segmental tunnel concrete lining and steel plates

	Young's modulus /MPa	Poisson's ratio	Yielding stress /MPa
C55 concrete	35.5	0.167	25.3
steel plates	2×10^5	0.2	215

753

754

755 Table 3 The stiffness values of the spring elements simulating the segmental joints

756 and epoxy bonding behaviour

Position	Direction	Symbol	stiffness (N/m)
segmental joints	radial	k_{j_r}	5×10^{8}
epoxy bonding	tangential	k_{b_θ}	3.74×10^{8}
	radial	k_{b_r}	3.45×10^{9}

757

758

759

760 Table 4 Comparison between the actual design and the optimal designs derived by the

761 robust retrofitting design methodology

Design Point	w_s **/mm**	t_s **/mm**	**std of** ΔD_{hs} **/mm**	**Cost / ×10^4**
1	850	30	1.800	15.571
2	950	27.5	1.624	15.625
3	750	27.5	1.767	13.388
4	700	17.5	2.324	9.982

762

763

764

765 Figure 1 Photograph of a steel plate reinforced segmental tunnel lining

766

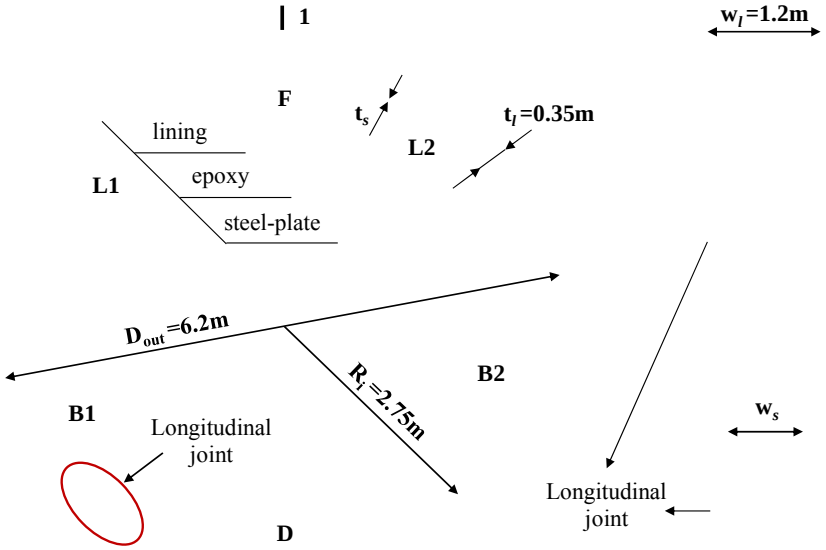

Figure 2 Diagram of showing an example of segmental tunnel linings reinforced by steel plates

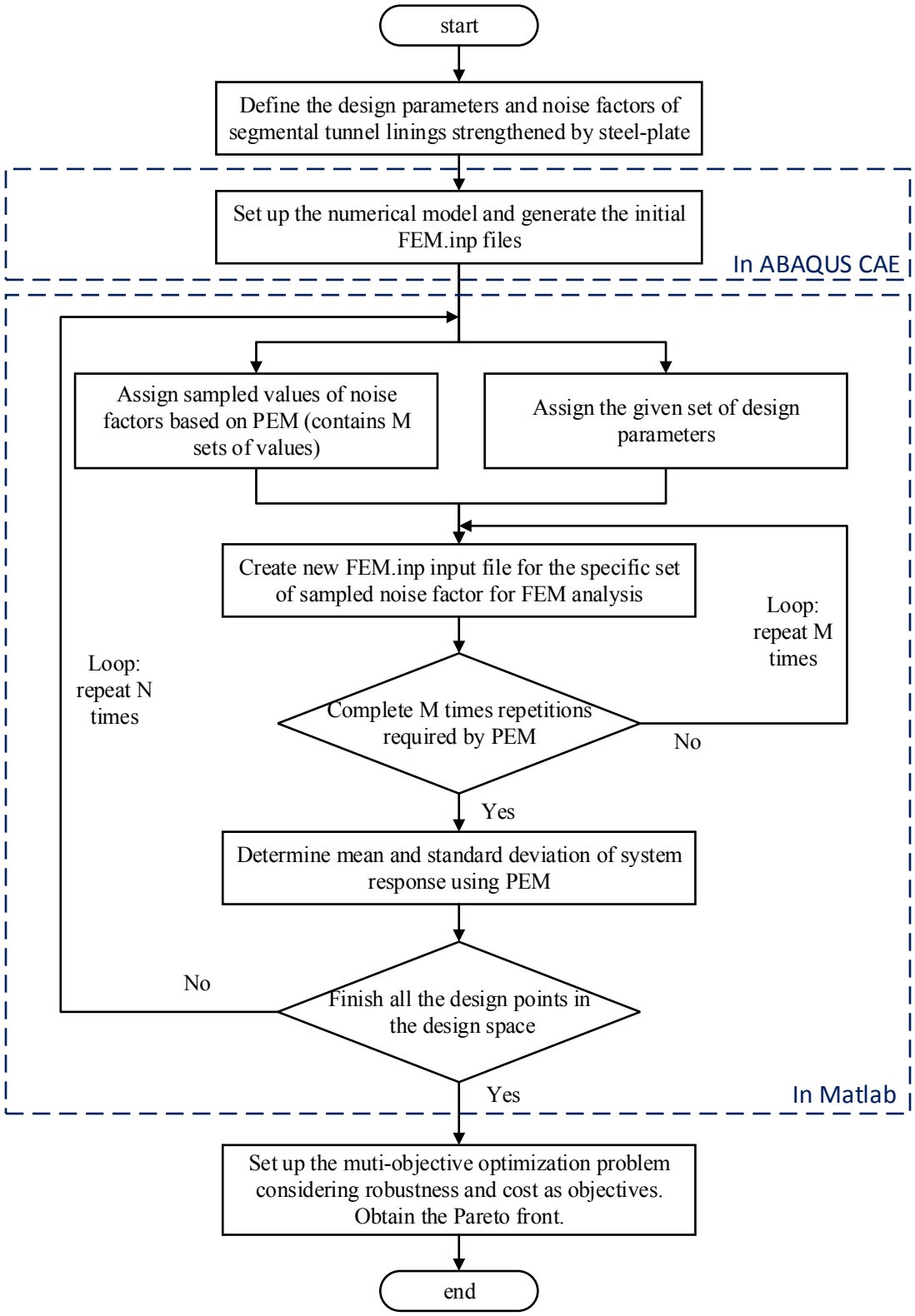

Figure 3 Flowchart for developing a robust retrofitting design

776

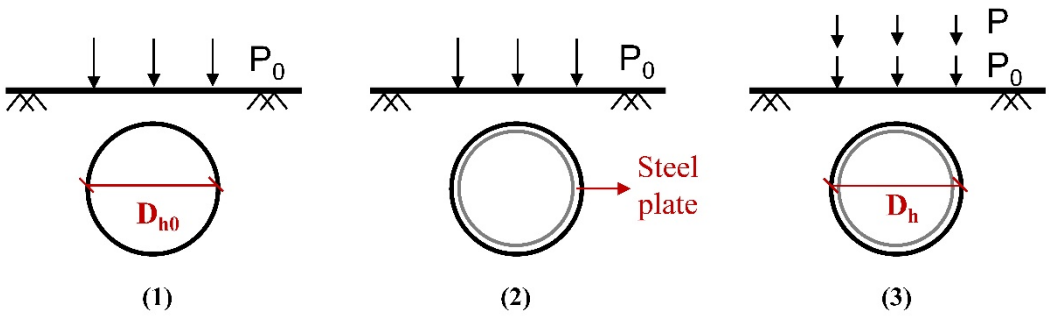

777

778 Figure 4 Numerical analysis procedure

779

780

Find value of design parameters:

w_s (width of reinforcing steel plate)

t_s (thickness of reinforcing steel plate)

Subjected to constraints:

$w_{sl} \leq w_s \leq w_{su}$

$t_{sl} \leq t_s \leq t_{su}$

$f_s > f_{sl}$

Objectives:

Maximizing the robustness index, R_s

Minimizing the cost, C

781

782 Figure 5 Multi-objective optimization formulation for robust retrofitting design

783

784

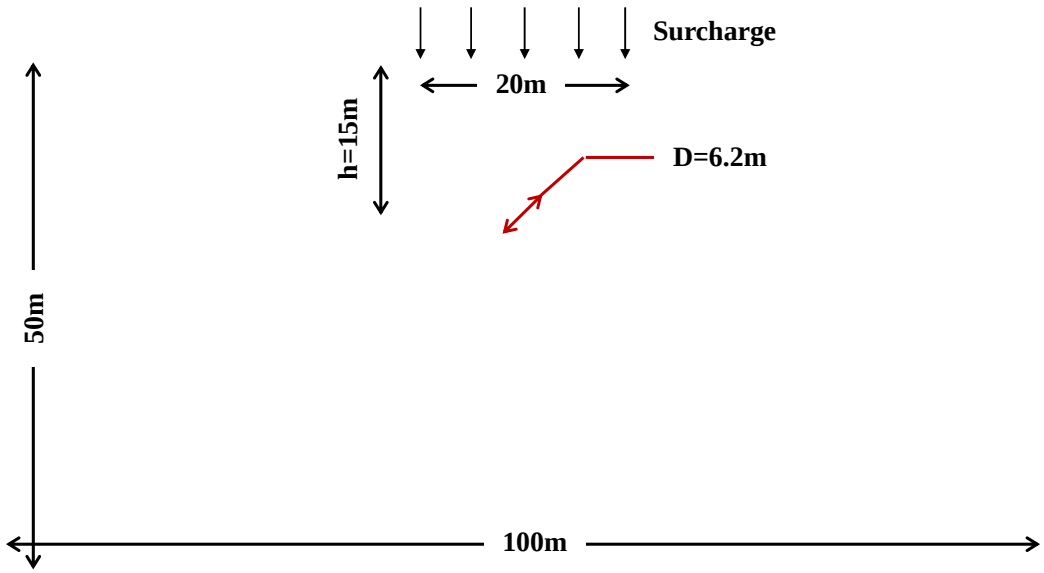

785

786 Figure 6 Finite element mesh for the ground

787

788

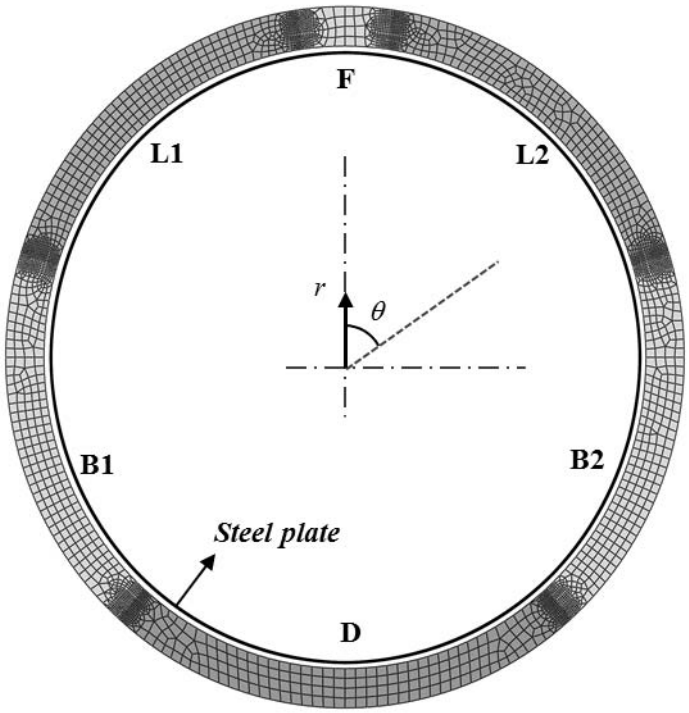

789

790 (a)

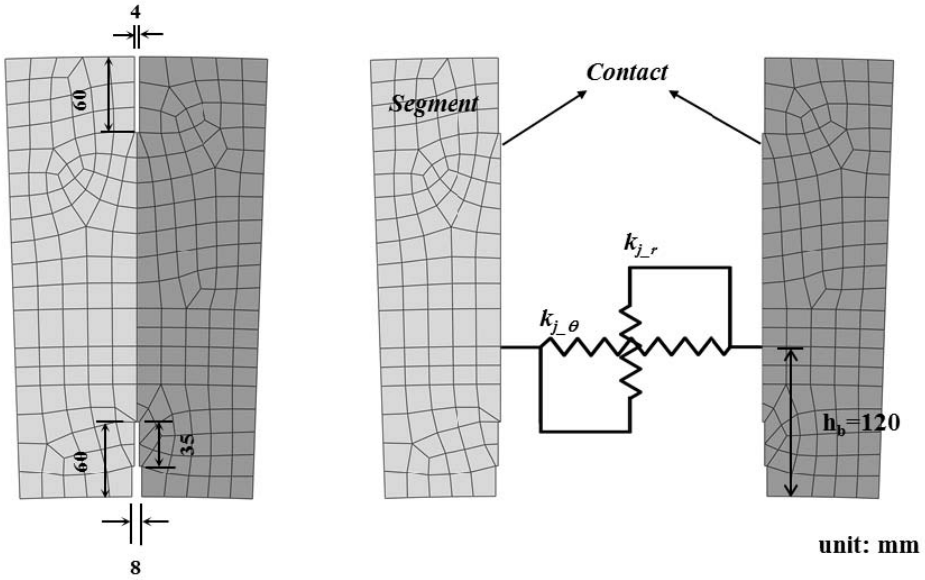

791

792 (b)

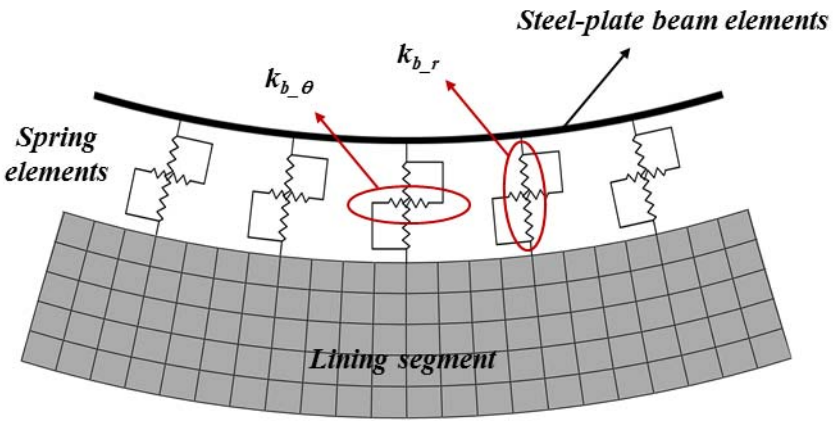

(c)

Figure 7 Finite element model for steel plates reinforced segmental linings, (a) the 2D model for the full reinforced tunnel lining, (b) the radial lining joint, (c) modelling the bond between the steel plates and the lining segment

799

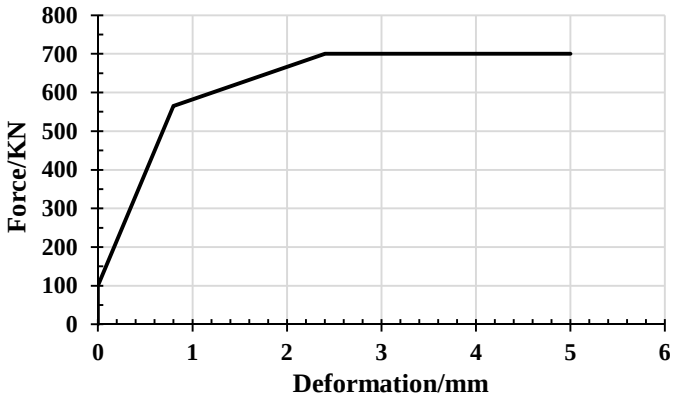

800

801 Figure 8 Force-deformation relationship assigned to tangential spring in the segment

802 joint

803

804

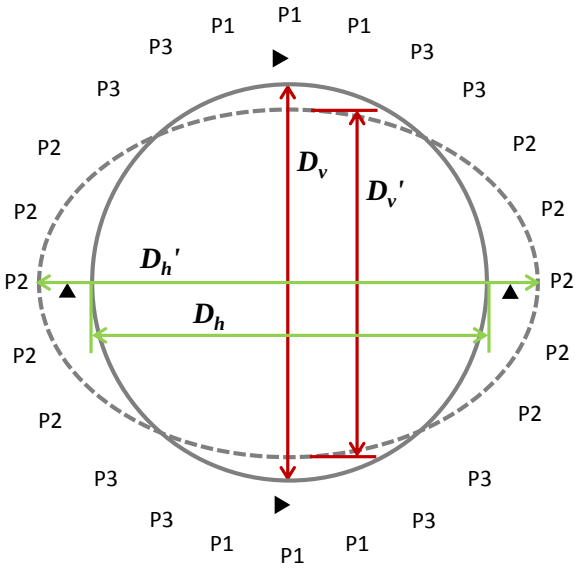

805

806 Figure 9 Schematic of the applied loading

807

808

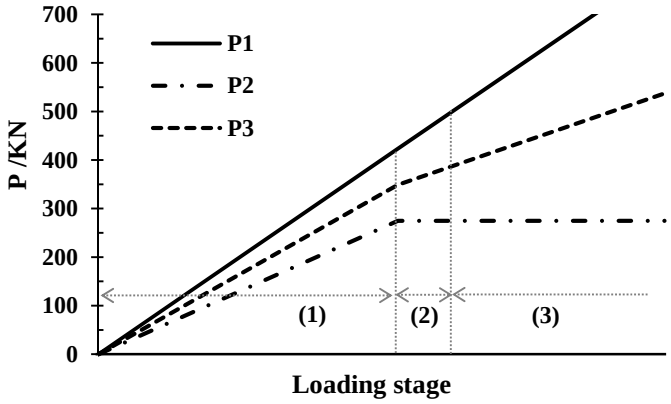

809

810 Figure 10 The loading process for P1, P2 and P3

811

812

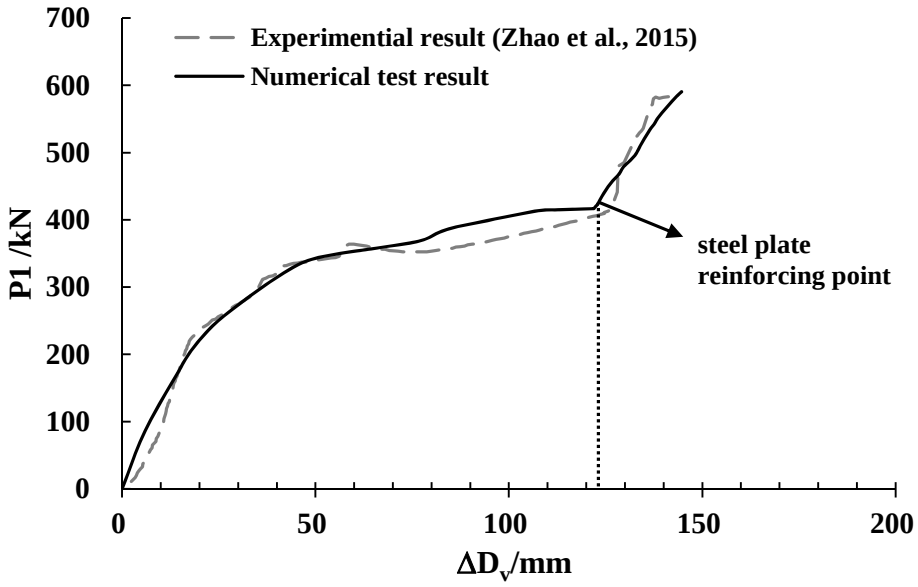

813

814 Figure 11 Comparison between the full-scale test results and the numerical analysis

815 results

816

817

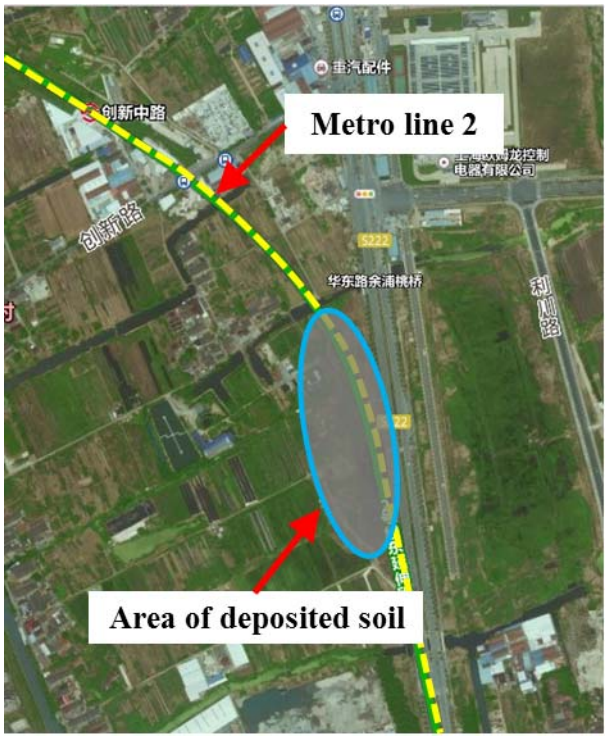

818

819 Figure 12 Location of the surcharge area (Huang et al., 2017)

820

821

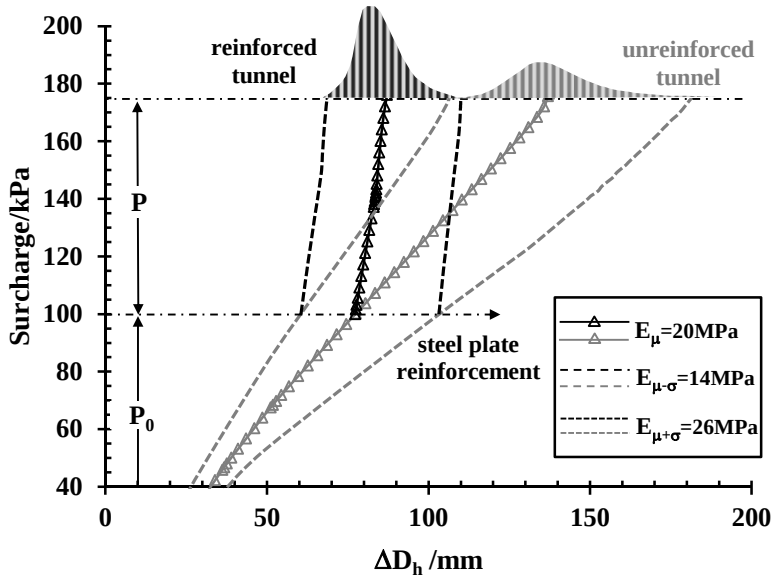

822

823 Figure 13 Curves showing the horizontal convergence (ΔD_h) against surcharge value

824

825

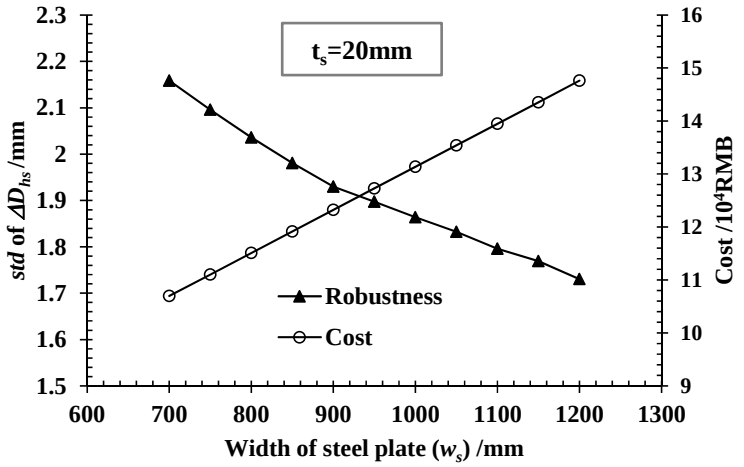

826

827 (a)

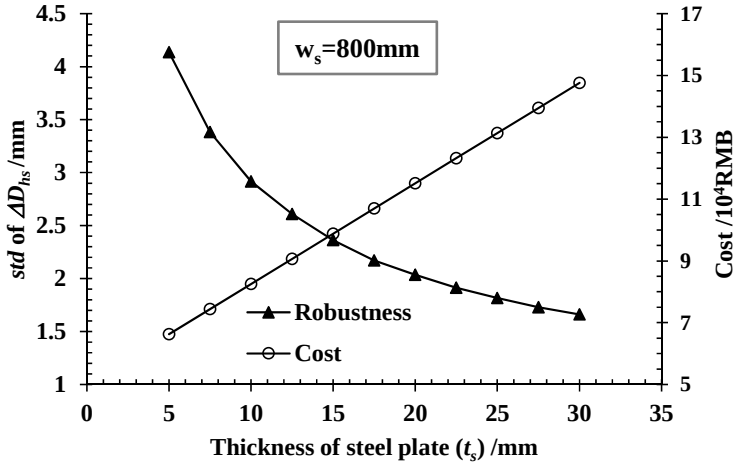

828

829 (b)

830 Figure 14 Influence of steel plate size on cost and robustness, (a) influence of steel

831 plate width (w_s), (b) influence of steel plate thickness (t_s)

832

833

Find value of design parameters:

w_s (width of reinforcing steel plate)

t_s (thickness of reinforcing steel plate)

unit:mm

Subjected to constraints:

$700 \leq w_s \leq 1200$ (with interval of 50)

$5 \leq t_s \leq 30$ (with interval of 2.5)

Safety factor $f_s > 1.5$

Objectives:

Minimizing the standard deviation of ΔD_{hs} (mm)

Minimizing the cost of steel plate reinforcement (RMB)

834

835 Figure 15 Formulation of the robust design for the rehabilitation of segmental tunnel

836 linings using steel plates

837

838

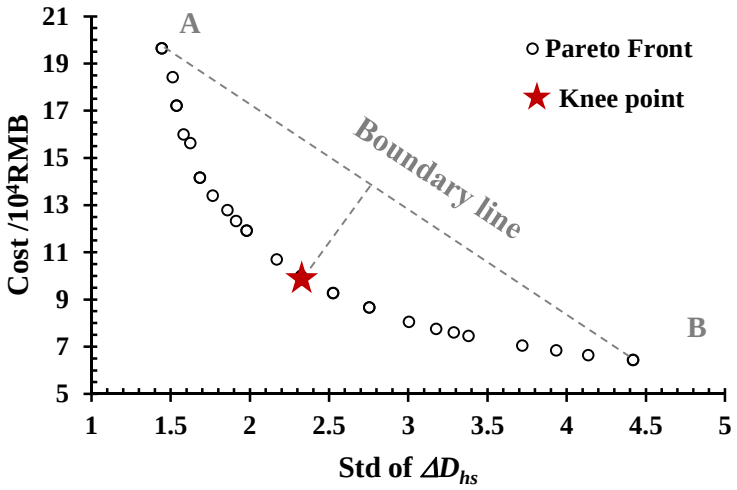

839

840 Figure 16 The Pareto Front obtained using NSGA-II

841

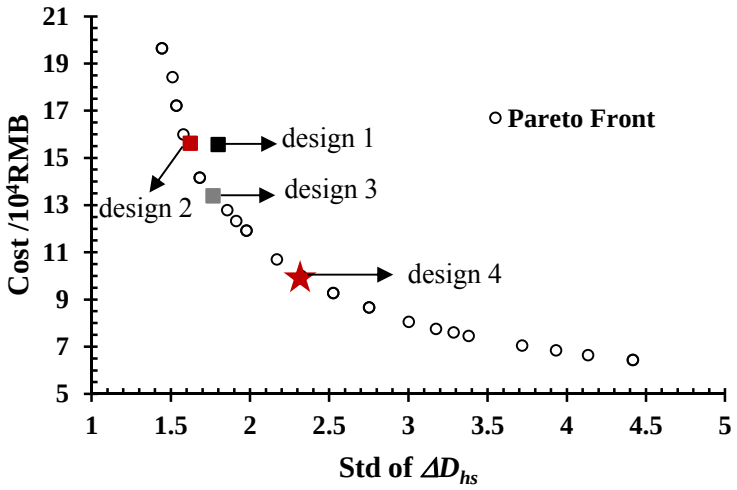

Figure 17 Comparison between the actual design and the optimal designs on the Pareto Front